

## Detecting the Higgs Bosons of Minimal Supergravity with Muon Pairs

V. Barger and Chung Kao

*Department of Physics, University of Wisconsin, Madison, WI 53706, USA*

### Abstract

The prospects at the CERN LHC are investigated for the discovery via decays into muon pairs of neutral Higgs bosons in the minimal supergravity model. Promising results are found for the CP-odd pseudoscalar ( $A^0$ ) and the heavier CP-even scalar ( $H^0$ ) Higgs bosons at large  $\tan\beta \equiv v_2/v_1$ . For  $\tan\beta \gtrsim 10$  and  $100 \text{ GeV} \lesssim m_A, m_H \lesssim 550 \text{ GeV}$ , the  $A^0$  and the  $H^0$  masses could be precisely reconstructed from the dimuon invariant mass.

## I. INTRODUCTION

In the Standard Model (SM) of electroweak interactions, the masses of gauge bosons and fermions are generated by a scalar field doublet. After spontaneous symmetry breaking, a neutral CP-even Higgs boson ( $h_{SM}^0$ ) remains as a physical particle. The scalar sector of the SM is unstable to radiative corrections that arise when the SM is coupled to ultraheavy degrees of freedom such as those in a grand unified theory (GUT). Therefore, there is great interest in extensions of the SM that can solve this problem.

A supersymmetry (SUSY) between fermions and bosons provides a natural explanation of the Higgs mechanism for electroweak symmetry breaking (EWSB) in the framework of a grand unified theory (GUT) and preserves the elementary nature of Higgs bosons. For the particle content of the minimal supersymmetric standard model (MSSM) [1], the evolution of gauge couplings by renormalization group equations (RGEs) [2] is consistent with a grand unified scale at  $M_{\text{GUT}} \sim 2 \times 10^{16}$  GeV and an effective SUSY mass scale in the range  $M_Z < M_{\text{SUSY}} \lesssim 10$  TeV [3]. With a large top quark Yukawa coupling ( $Y_t$ ) to a Higgs boson at the GUT scale, radiative corrections drive the corresponding Higgs boson mass squared parameter negative, spontaneously breaking the electroweak symmetry and naturally explaining the origin of the electroweak scale. In the minimal supersymmetric GUT with a large  $Y_t$ , there is an infrared fixed point (IRFP) [4,5] at low  $\tan\beta$ ; the top quark mass is correspondingly predicted to be  $m_t = (200 \text{ GeV}) \sin\beta$  [4], and thus  $\tan\beta \simeq 1.8$  for  $m_t = 175$  GeV. At high  $\tan\beta$ , another quasi-IRFP solution ( $dY_t/dt \simeq 0$ ) exists at  $\tan\beta \sim 56$ .

The Higgs sector of a supersymmetric theory must contain at least two  $SU(2)$  doublets [6] for anomaly cancellation. In the minimal supersymmetric standard model (MSSM), the Higgs sector has two doublets  $\phi_1$  and  $\phi_2$  that couple to the  $t_3 = -1/2$  and  $t_3 = +1/2$  fermions, respectively. After spontaneous symmetry breaking, there remain five physical Higgs bosons: a pair of singly charged Higgs bosons  $H^\pm$ , two neutral CP-even scalars  $H^0$  (heavier) and  $h^0$  (lighter), and a neutral CP-odd pseudoscalar  $A^0$ . The Higgs potential is constrained by supersymmetry such that all tree-level Higgs boson masses and couplings are determined by just two independent parameters, commonly chosen to be the mass of the CP-odd pseudoscalar ( $m_A$ ) and the ratio of vacuum expectation values (VEVs) of Higgs fields ( $\tan\beta \equiv v_2/v_1$ ).

Extensive studies have been made of the prospects for the detection of MSSM Higgs bosons at the LHC [7–13]. Most studies have focused on the SM decay modes  $\phi \rightarrow \gamma\gamma$  ( $\phi = H^0, h^0$  or  $A^0$ ) and  $\phi \rightarrow ZZ$  or  $ZZ^* \rightarrow 4l$  ( $\phi = H^0$  or  $h^0$ ) that are detectable above background. For  $\tan\beta$  close to one, the detection modes  $A^0 \rightarrow Zh^0 \rightarrow l^+l^-b\bar{b}$  or  $l^+l^-\tau\bar{\tau}$  [14] and  $H^0 \rightarrow h^0h^0 \rightarrow \gamma\gamma b\bar{b}$  [13] may provide promising channels to simultaneously discover two Higgs bosons of the MSSM. There are regions of parameter space where rates for Higgs boson decays to SUSY particles are large and dominant. While these decays reduce the rates for the standard modes, making conventional detection of Higgs bosons more difficult, they also open up a number of new promising modes for Higgs detection [10].

For large  $\tan\beta$ , the  $\tau\bar{\tau}$  decay mode [9,11,12] is a promising discovery channel for the  $A^0$  and the  $H^0$  in the MSSM. It was also suggested that neutral Higgs bosons might be observable via their  $b\bar{b}$  decays [15,16] in a large region of the  $(m_A, \tan\beta)$  plane, provided that sufficient  $b$ -tagging capability can be achieved. However, simulations with ATLAS detector performance concluded that detection of the  $b\bar{b}$  channel would be difficult [17].

Recently, the muon pair decay mode was proposed [18,11] and confirmed [13] to be a promising discovery channel for the  $A^0$  and the  $H^0$ . Although the  $\mu\bar{\mu}$  channel has a small branching fraction, this is compensated by the much better achievable mass resolution with muon pairs. For large  $\tan\beta$ , the muon pair discovery mode might be the only channel at the LHC that allows precise reconstruction of the  $A^0$  and the  $H^0$  masses.

In supergravity (SUGRA) models [19], supersymmetry is broken in a hidden sector with SUSY breaking communicated to the observable sector through gravitational interactions, leading naturally but not necessarily [20] to a common scalar mass ( $m_0$ ), a common gaugino mass ( $m_{1/2}$ ), a common trilinear coupling ( $A_0$ ) and a common bilinear coupling ( $B_0$ ) at the GUT scale. Through minimization of the Higgs potential, the  $B$  coupling parameter of the superpotential and the magnitude of the Higgs mixing parameter  $\mu$  are related to the ratio of VEVs of Higgs fields ( $\tan\beta \equiv v_2/v_1$ ) and to the mass of the  $Z$  boson ( $M_Z$ ). The SUSY particle masses and couplings at the weak scale can be predicted by the evolution of RGEs from the unification scale [4,21].

For  $\tan\beta$  close to 1.8, the lower IRFP, masses of the CP-odd pseudoscalar ( $m_A$ ) and the heavier CP-even scalar ( $m_H$ ) are large over most of the minimal supergravity parameter space. Then the couplings of the lighter scalar  $h^0$  are similar to those of the SM Higgs boson; the  $h^0$  could be the only neutral Higgs boson observable at the CERN LHC. For large  $\tan\beta$ , the  $A^0$  and the  $H^0$  can become light [22,23] and potentially visible at the LHC.

Recent measurements of the  $b \rightarrow s\gamma$  decay rate by the CLEO [24] and LEP collaborations [25] place constraints on the parameter space of the minimal supergravity model [26]. It was found that  $b \rightarrow s\gamma$  excludes most of the minimal supergravity (mSUGRA) parameter space when  $\tan\beta$  is large and  $\mu > 0$  [26]. Therefore, we will choose  $\mu < 0$  in our analysis. However, our results are almost independent of the sign of  $\mu$ .

The remainder of this article addresses the prospects of discovering the neutral Higgs bosons in the mSUGRA model via their decays into muon pairs at the LHC. The cross section and branching fractions are presented in Section II. The observability of the dimuon signals is discussed in Section III for conservative assumption about the detector mass resolution. Promising conclusions are drawn in Section IV.

## II. CROSS SECTION AND BRANCHING FRACTION

We evaluate SUSY mass spectra and couplings in the minimal supergravity model with four parameters:  $m_0$ ,  $m_{1/2}$ ,  $A_0$  and  $\tan\beta$ , and with the sign of the Higgs mixing parameter  $\mu$ . Since  $A_0$  mainly affects the masses of third generation sfermions, which do not significantly affect our analysis, we take  $A_0 = 0$  in our calculations.

The mass matrix of the charginos in the weak eigenstates ( $\tilde{W}^\pm$ ,  $\tilde{H}^\pm$ ) has the following form [4]

$$M_C = \begin{pmatrix} M_2 & \sqrt{2}M_W \sin\beta \\ \sqrt{2}M_W \cos\beta & -\mu \end{pmatrix}. \quad (1)$$

This mass matrix is not symmetric and must be diagonalized by two matrices [1]. The sign of the  $\mu$  contribution in Eq. (1) establishes our sign convention for  $\mu$ .

We calculate the masses and couplings in the Higgs sector with one-loop corrections from both the top and the bottom Yukawa interactions in the RGE-improved one-loop

effective potential [27] at the scale  $Q = \sqrt{m_{\tilde{t}_L} m_{\tilde{t}_R}}$ . With this scale choice, the numerical value of the CP-odd Higgs boson mass ( $m_A$ ) at large  $\tan\beta$  [22,23] is relatively insensitive to the exact scale choice and the loop corrections to  $m_A$  are small compared to the tree level contribution. In addition, when this high scale is used, the RGE improved one-loop corrections approximately reproduce the dominant two-loop perturbative calculation of the mass of the lighter CP-even Higgs scalar ( $m_h$ ). Our numerical values of  $m_h$  are very close to the results of Ref. [28] where somewhat different scales higher than  $M_Z$  have been adopted in evaluating the effective potential.

The cross section of  $pp \rightarrow \phi \rightarrow \mu\bar{\mu} + X$  ( $\phi = A^0, H^0$ , or  $h^0$ ) is calculated for the two dominant subprocesses  $gg \rightarrow \phi$  and  $gg \rightarrow \phi b\bar{b}$ , and multiplied by the branching fraction of the Higgs decay into muon pairs  $B(\phi \rightarrow \mu\bar{\mu})$ . The parton distribution functions of CTEQ3L [29] are used to evaluate the  $pp \rightarrow \phi + X$  cross section with  $\Lambda_4 = 0.177$  GeV and  $Q = M_{gg}$  = the invariant mass of the gluons. We take  $M_Z = 91.19$  GeV,  $\sin^2 \theta_W = 0.2319$ ,  $M_W = M_Z \cos \theta_W$ ,  $m_b(\text{pole}) = 4.8$  GeV, and  $m_t(\text{pole}) = 175$  GeV.

At the LHC energy, the SM Higgs boson is produced dominantly from gluon fusion; vector boson fusion is also relevant if the Higgs boson is heavy. In the MSSM, gluon fusion ( $gg \rightarrow \phi$ ) is the major source of neutral Higgs bosons for  $\tan\beta$  less than about 4. If  $\tan\beta$  is larger than about 10, neutral Higgs bosons in the MSSM are dominantly produced from  $b$ -quark fusion ( $b\bar{b} \rightarrow \phi$ ) [30]. The cross section of  $gg \rightarrow \phi b\bar{b}$  is a good approximation to the ‘exact’ cross section [30] of  $b\bar{b} \rightarrow \phi$  for  $M_\phi$  less than about 500 GeV. Since the Yukawa couplings of  $\phi b\bar{b}$  are enhanced by  $1/\cos\beta$ , the production rate of neutral Higgs bosons is usually enhanced at large  $\tan\beta$ . For  $m_A$  larger than about 150 GeV, the couplings of the lighter scalar  $h^0$  to gauge bosons and fermions become similar to those of the SM Higgs boson. Then gluon fusion is the major source of the  $h^0$  even if  $\tan\beta$  is large.

The QCD radiative corrections to the subprocess  $gg \rightarrow \phi$  are substantial [31,32]; the corrections to  $gg \rightarrow \phi b\bar{b}$  are still to be evaluated. To be conservative, we take a K-factor of 1.5 for the contribution from  $gg \rightarrow \phi$  and a K-factor of 1.0 for the contribution from  $gg \rightarrow \phi b\bar{b}$ . For the dominant Drell-Yan background [18,11,13], we adopt the well known K-factor from reference [33].

With QCD radiative corrections to  $\phi \rightarrow b\bar{b}$  [34], the branching fraction of  $\phi \rightarrow \mu\bar{\mu}$  is about  $m_\mu^2/3m_b^2(m_b) \sim 2 \times 10^{-4}$  when the  $b\bar{b}$  mode dominates Higgs decays, where 3 is a color factor of the quarks and  $m_b(m_b)$  is the running mass at the scale  $m_b$ . The branching fraction of  $h^0 \rightarrow \mu\bar{\mu}$  is always about  $2 \times 10^{-4}$ . The branching fractions for  $A^0 \rightarrow \mu\bar{\mu}$  and  $H^0 \rightarrow \mu\bar{\mu}$  are always in the range  $1.5 - 2.5 \times 10^{-4}$  when  $\tan\beta \gtrsim 10$ , even when  $A^0$  and  $H^0$  can decay into SUSY particles. For  $m_A$  less than about 80 GeV, the  $H^0$  decays dominantly into  $h^0 h^0$ ,  $A^0 A^0$  and  $ZA^0$ .

In Figures 1(a) and 1(b), we present the cross section of the MSSM Higgs bosons at the LHC,  $pp \rightarrow \phi \rightarrow \mu\bar{\mu} + X$ , as a function of  $m_A$  for  $m_{\tilde{q}} = m_{\tilde{g}} = -\mu = 1$  TeV, (a)  $\tan\beta = 15$  and (b)  $\tan\beta = 40$ . As  $\tan\beta$  increases, the production cross section is enhanced because for  $\tan\beta \gtrsim 10$ , the production cross section is dominated by  $gg \rightarrow \phi b\bar{b}$  and enhanced by the  $\phi b\bar{b}$  Yukawa coupling. Also shown is the same cross section for the SM Higgs boson  $h_{SM}^0$  with  $m_{h_{SM}} = m_A$ . For  $m_{h_{SM}} > 140$  GeV, the SM  $h_{SM}^0$  mainly decays into gauge bosons, and the branching fraction  $B(h_{SM}^0 \rightarrow \mu\bar{\mu})$  drops sharply in this mass region.

We present the cross section of  $pp \rightarrow \phi \rightarrow \mu\bar{\mu} + X$  as a function of  $\tan\beta$  for  $\mu < 0$ ,  $m_0 = 300$  GeV and various values of  $m_{1/2}$  in Figure 2. The regions in Fig. 2 with dark

shading denote the parts of the parameter space that do not have the lightest neutralino ( $\chi_1^0$ ) as the lightest supersymmetric particle (LSP). As  $\tan\beta$  increases, the production cross section is enhanced because (i)  $m_A$  is reduced; and (ii) for  $\tan\beta \gtrsim 10$ , the production cross section is enhanced by the  $\phi b\bar{b}$  Yukawa coupling. Also shown in Fig. 2 are the pseudoscalar mass ( $m_A$ ) versus  $\tan\beta$  and the invariant mass distribution ( $d\sigma/dM_{\mu\bar{\mu}}$ ) of the background from the Drell-Yan process at  $M_{\mu\bar{\mu}} = m_A$ .

In Figure 3, we show the cross section of  $pp \rightarrow \phi \rightarrow \mu\bar{\mu} + X$  in fb, as a function of  $m_{1/2}$ , with  $\sqrt{s} = 14$  TeV, for  $\mu > 0$ ,  $m_0 = 300$  GeV, and (a)  $\tan\beta = 1.8$ , (b)  $\tan\beta = 10$ , (c)  $\tan\beta = 35$ , and (d)  $\tan\beta = 50$ . Also shown are  $m_A$  versus  $m_{1/2}$  and the invariant mass distribution ( $d\sigma/dM_{\mu\bar{\mu}}$ ) of the background from the Drell-Yan process at  $M_{\mu\bar{\mu}} = m_A$ . The regions in Fig. 3 with dark shading denote the parts of the parameter space that do not satisfy the following theoretical requirements: tachyon free, and the lightest neutralino as the LSP. For  $\tan\beta \sim 1.8$ ,  $m_A$  is very large and the cross section of the  $A^0, H^0$  signal is much smaller than the background. For  $\tan\beta \gtrsim 35$ , the cross section of the  $A^0, H^0$  signal is greatly enhanced and can become slightly larger than the background. For  $\tan\beta \sim 50$  and  $m_{1/2} < 200$  GeV,  $m_A$  can become close to  $m_Z$  and a peak appears in the invariant mass distribution of the background from the Drell-Yan process.

### III. OBSERVABILITY AT THE LHC

We define the signal to be observable if the  $N\sigma$  lower limit on the signal plus background is larger than the corresponding upper limit on the background [7,36], namely,

$$L(\sigma_s + \sigma_b) - N\sqrt{L(\sigma_s + \sigma_b)} > L\sigma_b + N\sqrt{L\sigma_b} \quad (2)$$

which corresponds to

$$\sigma_s > \frac{N^2}{L} \left[ 1 + 2\sqrt{L\sigma_b}/N \right] \quad (3)$$

Here  $L$  is the integrated luminosity,  $\sigma_s$  is the cross section of Higgs signal, and  $\sigma_b$  is the background cross section within a bin of width  $\pm\Delta M_{\mu\bar{\mu}}$  centered at  $M_\phi$ ;  $N = 2.32$  corresponds to a 99% confidence level and  $N = 2.5$  corresponds to a  $5\sigma$  signal. We take the integrated luminosity  $L$  to be  $300 \text{ fb}^{-1}$  [13].

To study the observability of the muon discovery mode, we consider the background from the Drell-Yan (DY) process,  $q\bar{q} \rightarrow Z, \gamma \rightarrow \mu\bar{\mu}$ , which is the dominant background. We take  $\Delta M_{\mu\bar{\mu}}$  to be the larger of the ATLAS muon mass resolution (about 2% of the Higgs bosons mass) [12,13] or the Higgs boson width. The CMS mass resolution will be better than 2% of  $m_\phi$  for  $m_\phi \lesssim 500$  GeV [11,18]. Therefore, the observability will be better for the CMS detector. The minimal cuts applied are (1)  $p_T(\mu) > 20$  GeV and (2)  $|\eta(\mu)| < 2.5$  for both the signal and background. For  $m_A \gtrsim 130$  GeV,  $m_A$  and  $m_H$  are almost degenerate while for  $m_A \lesssim 100$  GeV  $m_A$  and  $m_h$  are very close to each other [18,11]. Therefore, we add up the cross sections of the  $A^0$  and the  $h^0$  for  $m_A \leq 100$  GeV and those of the  $A^0$  and the  $H^0$  for  $m_A > 100$  GeV.

The  $5\sigma$  discovery contours for the MSSM Higgs bosons at  $\sqrt{s} = 14$  TeV with an integrated luminosity  $L = 300 \text{ fb}^{-1}$  are shown in Figs. 1(c) and 1(d) for  $m_{\tilde{q}} = m_{\tilde{g}} = -\mu = 1$  TeV

and  $m_{\tilde{q}} = m_{\tilde{g}} = -\mu = 300$  GeV. The discovery region of  $H^0 \rightarrow \mu\bar{\mu}$  is slightly enlarged for a smaller  $m_A$ , but the observable region of  $h^0 \rightarrow \mu\bar{\mu}$  is slightly reduced because the lighter top squarks make the  $H^0$  and the  $h^0$  lighter; also the  $H^0 b\bar{b}$  coupling is enhanced while the  $h^0 b\bar{b}$  coupling is reduced.

In Figure 4, we present the LHC discovery contours in the minimal supergravity model, for (a) the  $m_{1/2}$  versus  $\tan\beta$  plane with  $m_0 = 150$  GeV, (b) the  $m_{1/2}$  versus  $\tan\beta$  plane with  $m_0 = 500$  GeV, (c) the  $m_{1/2}$  versus  $m_0$  plane with  $\tan\beta = 15$ , and (d) the  $m_{1/2}$  versus  $m_0$  plane with  $\tan\beta = 40$ . The discovery region is the part of the parameter space between the curve of square symbol and the dash line. The QCD radiative corrections to background from the Drell-Yan process are included. The regions in Fig. 4 with dark shading denote the parts of the parameter space that do not satisfy the following theoretical requirements: electroweak symmetry breaking (EWSB), tachyon free, and the lightest neutralino as the LSP. Also shown are the mass contours for  $m_A = 100$  GeV (dashed), 500 GeV (solid) and 1000 GeV (dot-dashed). For  $\tan\beta \gtrsim 40$ , it should be possible to observe the  $A^0$  or the  $H^0$  with a mass up to about 550 GeV.

There are a couple of interesting points to note: (i) an increase in  $\tan\beta$  leads to a larger  $m_h$  but a reduction in  $m_A$  and  $m_H$ ; (ii) an increase in  $m_0$  or in  $m_{1/2}$  raises  $m_A$ ,  $m_H$  and masses of the other scalars significantly.

#### IV. CONCLUSIONS

The muon pair decay mode is a very promising channel to discover the neutral Higgs bosons of minimal supersymmetry and minimal supergravity. The discovery region of the  $\mu\bar{\mu}$  mode is slightly smaller than the  $\tau\bar{\tau}$  channel but  $\mu\bar{\mu}$  allows precise reconstruction of the Higgs boson masses. The  $A^0$  and  $H^0$  should be observable in a large region of parameter space with  $\tan\beta \gtrsim 10$ . The  $h^0$  should be observable in a region with  $m_A < 120$  GeV and  $\tan\beta \gtrsim 5$ .

The observable regions of the parameter space are found to be

$$\begin{aligned} m_0 = 150 \text{ GeV} : \quad m_{1/2} &\lesssim 400 \text{ GeV and } \tan\beta \gtrsim 12 \\ m_0 = 500 \text{ GeV} : \quad m_{1/2} &\lesssim 1 \text{ TeV and } \tan\beta \gtrsim 28 \end{aligned} \quad (4)$$

For two specific choices of large  $\tan\beta$ , the observable regions are

$$\begin{aligned} \tan\beta = 15 : \quad m_{1/2} &\lesssim 200 \text{ GeV and } m_0 \lesssim 200 \text{ GeV} \\ \tan\beta = 40 : \quad m_{1/2} &\lesssim 600 \text{ GeV and } m_0 \lesssim 800 \text{ GeV} \end{aligned} \quad (5)$$

All observable regions are nearly independent of the sign of  $\mu$ .

For  $m_A \gtrsim 200$  GeV and  $\tan\beta > 25$ ,  $L = 10 \text{ fb}^{-1}$  would be sufficient [18] to obtain Higgs boson signals with a statistical significance larger than 7. For  $M_{\mu\bar{\mu}}$  close to the  $M_Z$ , the signal is marginal because it appears on the shoulder of the huge  $Z$  peak. Adequate subtraction procedures are required to extract the signal in this region.

#### ACKNOWLEDGMENTS

We are grateful to Nikita Stepanov for beneficial discussions. This research was supported in part by the U.S. Department of Energy under Grant No. DE-FG02-95ER40896 and in part

by the University of Wisconsin Research Committee with funds granted by the Wisconsin Alumni Research Foundation.

## REFERENCES

- [1] H.P. Nilles, Phys. Rep. **110** (1984) 1; H. Haber and G. Kane, Phys. Rep. **117** (1985) 75.
- [2] K. Inoue, A. Kakuto, H. Komatsu and H. Takeshita, Prog. Theor. Phys. **68** (1982) 927 and **71** (1984) 413.
- [3] P. Langacker and M. Luo, Phys. Rev. **D44** (1991) 817; J. Ellis, S. Kelley and D. Nanopoulos, Phys. Lett. **B260** (1991) 131; U. Amaldi, W. de Boer and H. Fürstenau, Phys. Lett. **B260** (1991) 447; R. Barbieri, talk given at the 18th International Symposium on Lepton-Photon Interactions, Hamburg, Germany, July 1997, hep-ph/9711232.
- [4] V. Barger, M.S. Berger, P. Ohmann, Phys. Rev. **D47** (1993) 1093; **D49** (1994) 4908; V. Barger, M.S. Berger, P. Ohmann and R.J.N. Phillips, Phys. Lett. **B314** (1993) 351.
- [5] B. Pendleton and G.G. Ross, Phys. Lett. **B98** (1981) 291; C.T. Hill, Phys. Rev. **D24** (1981) 691; C.D. Froggatt, R.G. Moorhouse and I.G. Knowles, Phys. Lett. **B298** (1993) 356; J. Bagger, S. Dimopoulos and E. Masso, Phys. Rev. Lett. **55** (1985) 920; H. Arason, *et al.*, Phys. Rev. Lett. **67** (1991) 2933; and Phys. Rev. **D46** (1992) 3945; P. Langacker, N. Polonsky, Phys. Rev. **D50** (1994) 2199; W.A. Bardeen, M. Carena, S. Pokorski and C.E.M. Wagner, Phys. Lett. **B320** (1994) 110; M. Carena, M. Olechowski, S. Pokorski and C.E.M. Wagner Nucl. Phys. **B419** (1994) 213; B. Schrempp, Phys. Lett. **B344** (1995) 193; B. Schrempp and M. Wimmer, DESY-96-109 (1996), hep-ph/9606386.
- [6] J. Gunion, H. Haber, G. Kane and S. Dawson, *The Higgs Hunter's Guide* (Addison-Wesley, Redwood City, CA, 1990).
- [7] H. Baer, M. Bisset, C. Kao and X. Tata, Phys. Rev. **D46** (1992) 1067.
- [8] V. Barger, M. Berger, A. Stange and R. Phillips, Phys. Rev. **D45** (1992) 4128; J. Gunion, R. Bork, H. Haber and A. Seiden, Phys. Rev. **D46**, 2040 (1992); J. Gunion, H. Haber and C. Kao, Phys. Rev. **D46**, 2907 (1992); J.F. Gunion and L. Orr, Phys. Rev. **D46** (1992) 2052.
- [9] Z. Kunszt and F. Zwirner, Nucl. Phys. **B385** (1992) 3.
- [10] H. Baer, M. Bisset, D. Dicus, C. Kao and X. Tata, Phys. Rev. **D47** (1993) 1062; H. Baer, M. Bisset, C. Kao and X. Tata, Phys. Rev. **D50** (1994) 316.
- [11] CMS Technical Proposal, CERN/LHCC 94-38 (1994).
- [12] Atlas Technical Proposal, CERN/LHCC 94-43 (1994).
- [13] E. Richter-Was, D. Froidevaux, F. Gianotti, L. Poggioli, D. Cavalli, and S. Resconi, CERN report CERN-TH-96-111, (1996).
- [14] S. Abdullin, H. Baer, C. Kao, N. Stepanov and X. Tata, Phys. Rev. **D54** (1996) 6728; H. Baer, C. Kao and X. Tata, Phys. Lett. **B303** (1993) 284.
- [15] T. Garavaglia, W. Kwong and D.-D. Wu, Phys. Rev. **D48**, 1899 (1993).
- [16] J. Dai, J.F. Gunion and R. Vega, Phys. Lett. **B315** (1993) 355; Phys. Lett. **B345** (1995) 29; **B387** (1996) 801.
- [17] E. Richter-Was and D. Froidevaux, CERN report CERN-TH-97-210, (1997), hep-ph/9708455.
- [18] C. Kao and N. Stepanov, Phys. Rev. D **52** (1995) 5025.

- [19] A.H. Chamseddine, R. Arnowitt and P. Nath, Phys. Rev. Lett. **49** (1982) 970; L. Ibañez and G. Ross, Phys. Lett. **B110** (1982) 215; L. Ibañez, Phys. Lett. **B118** (1982) 73; J. Ellis, D. Nanopoulos and K. Tamvakis, Phys. Lett. **B121** (1983) 123; L. Alvarez-Gaumé, J. Polchinski and M. Wise, Nucl. Phys. **B121** (1983) 495.
- [20] V. Berezhinskii et al., Astropart. Phys. **5** (1996) 1; P. Nath and R. Arnowitt, Northeastern Report No. NUB-TH-3151-97, (1997), hep-ph/9701301.
- [21] J. Ellis and F. Zwirner, Nucl. Phys. **B338** (1990) 317; G. Ross and R.G. Roberts, Nucl. Phys. **B377** (1992) 571; R. Arnowitt and P. Nath, Phys. Rev. Lett. **69** (1992) 725; M. Drees and M.M. Nojiri, Nucl. Phys. **B369** (1993) 54; S. Kelley *et. al.*, Nucl. Phys. **B398** (1993) 3; M. Olechowski and S. Pokorski, Nucl. Phys. **B404** (1993) 590; G. Kane, C. Kolda, L. Roszkowski and J. Wells, Phys. Rev. **D49** (1994) 6173; D.J. Castaño, E. Piard and P. Ramond, Phys. Rev. **D49** (1994) 4882; W. de Boer, R. Ehret and D. Kazakov, Z. Phys. **67** (1995) 647; H. Baer, M. Drees, C. Kao, M. Nojiri and X. Tata, Phys. Rev. D **50** (1994) 2148; H. Baer, C.-H. Chen, R. Munroe, F. Paige and X. Tata, Phys. Rev. D **51** (1995) 1046.
- [22] H. Baer, C.-H. Chen, M. Drees, F. Paige and X. Tata, Phys. Rev. Lett. **79** (1997) 986.
- [23] V. Barger and C. Kao, University of Wisconsin report, MADPH-97-992, (1997), hep-ph/9704403.
- [24] M.S. Alam et al., (CLEO Collaboration), Phys. Rev. Lett. **74** (1995) 2885.
- [25] P.G. Colrain and M.I. Williams, talk presented at the International Europhysics Conference on High Energy Physics, Jerusalem, Israel, August 1997.
- [26] P. Nath and R. Arnowitt, Phys. Lett. **B336** (1994) 395; Phys. Rev. Lett. **74** (1995) 4592; Phys. Rev. **D54** (1996) 2374; F. Borzumati, M. Drees and M. Nojiri, Phys. Rev. **D51** (1995) 341; H. Baer and M. Brhlik, Phys. Rev. **D55** (1997) 3201.
- [27] H. Haber and R. Hempfling, Phys. Rev. Lett. **66** (1991) 1815; J. Ellis, G. Ridolfi and F. Zwirner, Phys. Lett. **B257** (1991) 83; T. Okada, H. Yamaguchi and T. Tanagida, Prog. Theor. Phys. Lett. **85** (1991) 1; We use the calculations of M. Bisset, Ph.D. thesis, University of Hawaii (1994).
- [28] M. Carena, J.R. Espinosa, M. Quiros, and C.E.M. Wagner, Phys. Lett. **B355** (1995) 209; M. Carena, M. Quiros, C.E.M. Wagner, Nucl. Phys. **B461** (1996) 407; H. Haber, R. Hempfling and A. Hoang, CERN-TH/95-216 (1996), hep-ph/9609331.
- [29] H.L. Lai et al., Phys. Rev. **D51** (1995) 4763.
- [30] D. Dicus and S. Willenbrock, Phys. Rev. **D39** (1989) 751.
- [31] S. Dawson, Nucl. Phys. **B359** (1991) 283; A. Djouadi, M. Spira and P.M. Zerwas, Phys. Lett. **B264** (1991) 440; D. Graudenz, M. Spira and P.M. Zerwas, Phys. Rev. Lett. **70** (1993) 1372; M. Spira, A. Djouadi, D. Graudenz and P.M. Zerwas, Nucl. Phys. **B453** (1995) 17.
- [32] S. Dawson, A. Djouadi and M. Spira, Phys. Rev. Lett. **77** (1996) 16.
- [33] V. Barger and R. Phillips, *Collider Physics, updated edition*, (Addison-Wesley Publishing Company, Redwood City, CA, 1997).
- [34] E. Braaten, J.P. Leveille, Phys. Rev. **D22** (1980) 715; M. Drees and K. Hikasa, Phys. Lett. **B240** (1990) 455; (E)-*ibid.* **B262** (1991) 497.
- [35] ALEPH collaboration, talk presented at CERN by G. Cowan, February, 1997.
- [36] N. Brown, Z. Phys. **C49** (1991) 657.



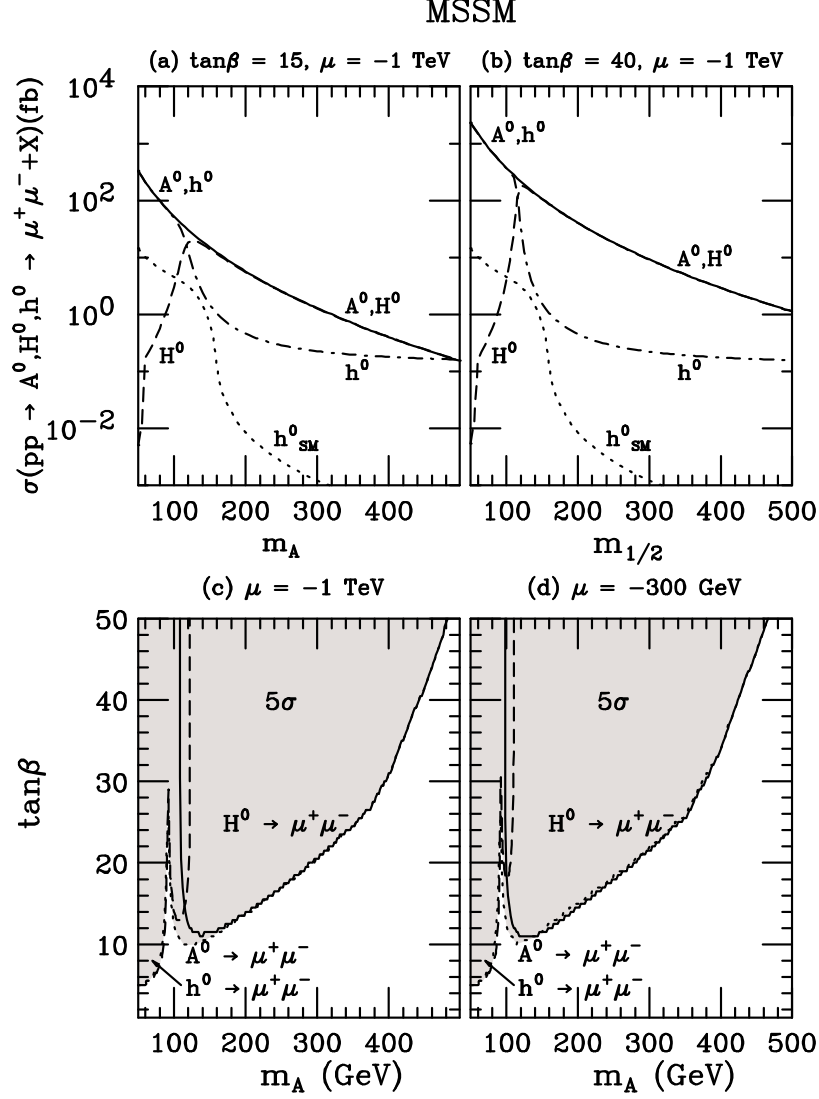


FIG. 1. The total cross section of  $pp \rightarrow A^0, H^0, h^0 \rightarrow \mu\bar{\mu} + X$  in fb at  $\sqrt{s} = 14$  TeV, as a function of  $m_A$  in the MSSM, for  $m_{\tilde{g}} = m_{\tilde{q}} = -\mu = 1$  TeV, (a)  $\tan\beta = 15$  and (b)  $\tan\beta = 40$ . Also shown are the cross section for the SM Higgs boson with  $m_{h_{SM}} = m_A$  (dotted). The 5 $\sigma$  contours at the LHC with  $L = 300$  fb $^{-1}$  are shown for (c)  $m_{\tilde{g}} = m_{\tilde{q}} = -\mu = 1$  TeV, and (d)  $m_{\tilde{g}} = m_{\tilde{q}} = -\mu = 300$  GeV. The discovery region is the part of the parameter space with light shading.

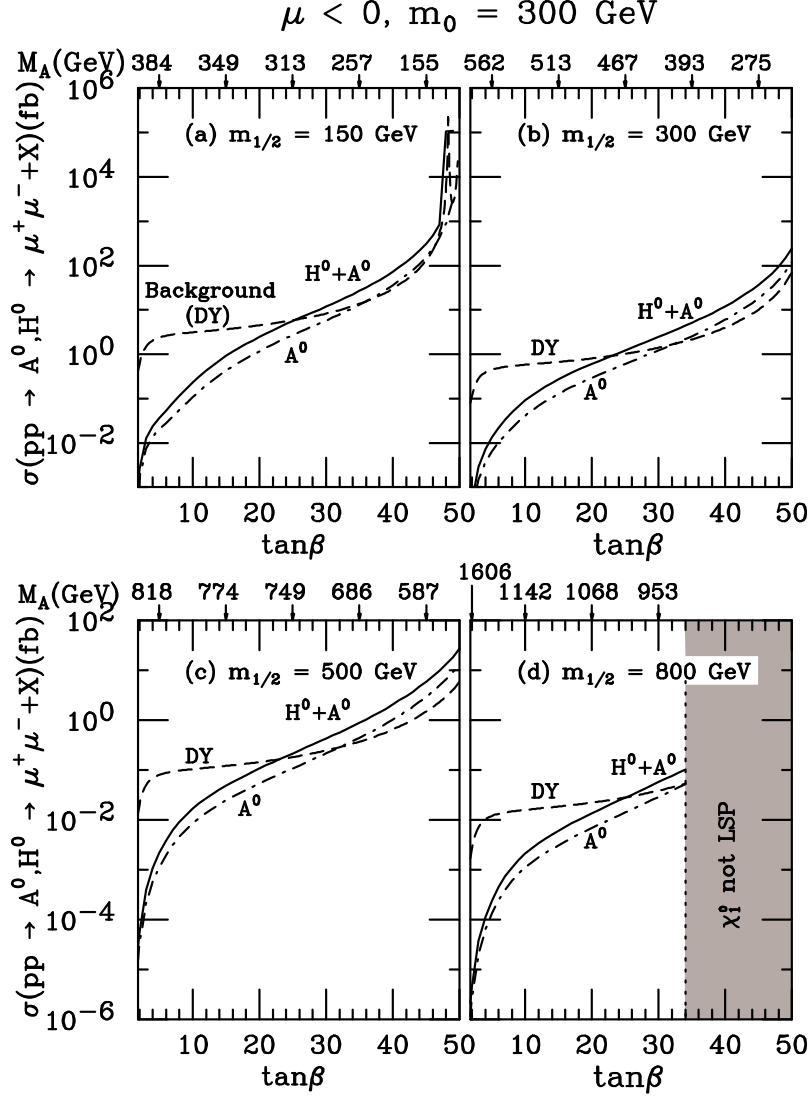


FIG. 2. The total cross section of  $pp \rightarrow A^0, H^0 \rightarrow \mu\bar{\mu} + X$  in fb at  $\sqrt{s} = 14 \text{ TeV}$ , as a function of  $\tan\beta$ , for  $\mu < 0$ ,  $m_0 = 300 \text{ GeV}$ , and (a)  $m_{1/2} = 150 \text{ GeV}$ , (b)  $m_{1/2} = 300 \text{ GeV}$ , (c)  $m_{1/2} = 500 \text{ GeV}$ , and, (d)  $m_{1/2} = 800 \text{ GeV}$ . Also shown is the invariant mass distribution ( $d\sigma/dM_{\mu\bar{\mu}}$ ) of the Drell-Yan background (dashed) in fb/GeV for  $M_{\mu\bar{\mu}} = m_A$ . The region with dark shading denotes the part of the parameter space that does not have the lightest neutralino ( $\chi_1^0$ ) as the LSP.

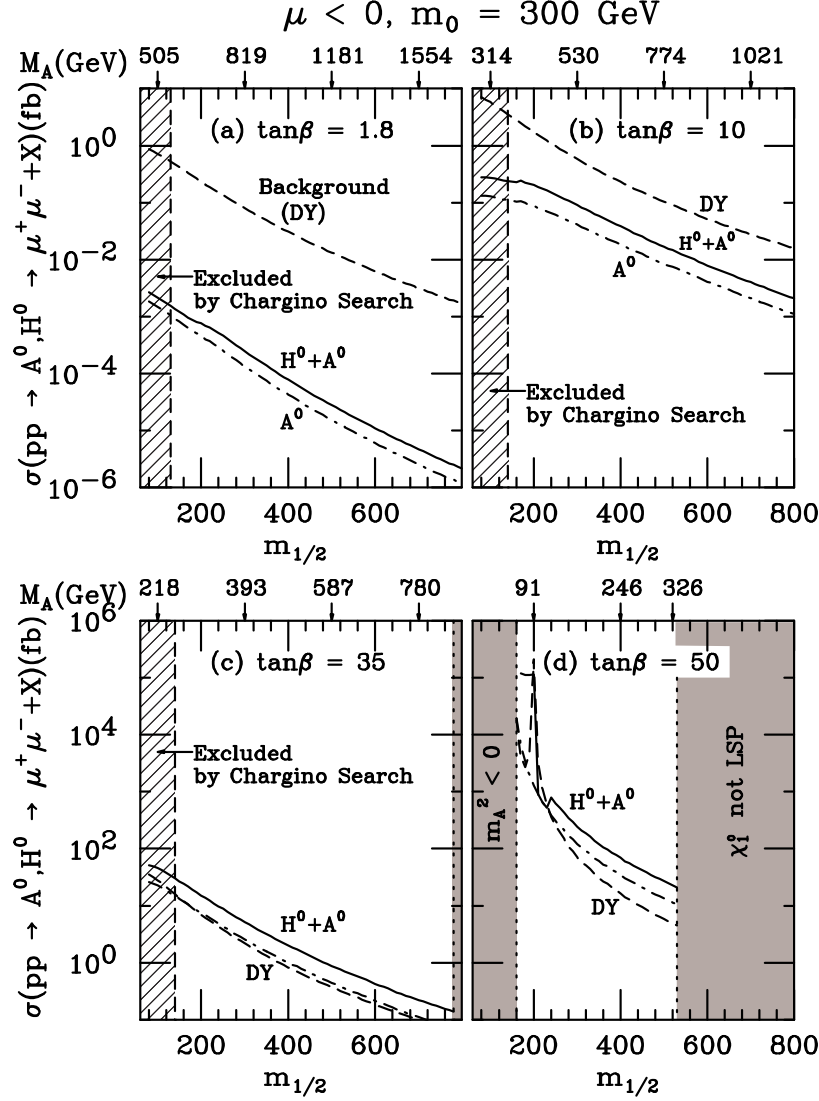


FIG. 3. The total cross section of  $pp \rightarrow A^0, H^0 \rightarrow \mu\bar{\mu} + X$  in fb at  $\sqrt{s} = 14$  TeV, as a function of  $m_{1/2}$ , for  $\mu < 0$ ,  $m_0 = 300$  GeV, (a)  $\tan\beta = 1.8$ , (b)  $\tan\beta = 10$ , (c)  $\tan\beta = 35$ , and (d)  $\tan\beta = 50$ . Also shown is  $d\sigma/dM_{\mu\bar{\mu}}$  of the Drell-Yan background (dashed) in (fb/GeV) for  $M_{\mu\bar{\mu}} = m_A$ . The regions with dark shading are the parts of the parameter space excluded by theoretical requirements. The region excluded by the  $m_{\chi_1^+} > 85$  GeV limit from the chargino search [35] at LEP 2 is indicated.

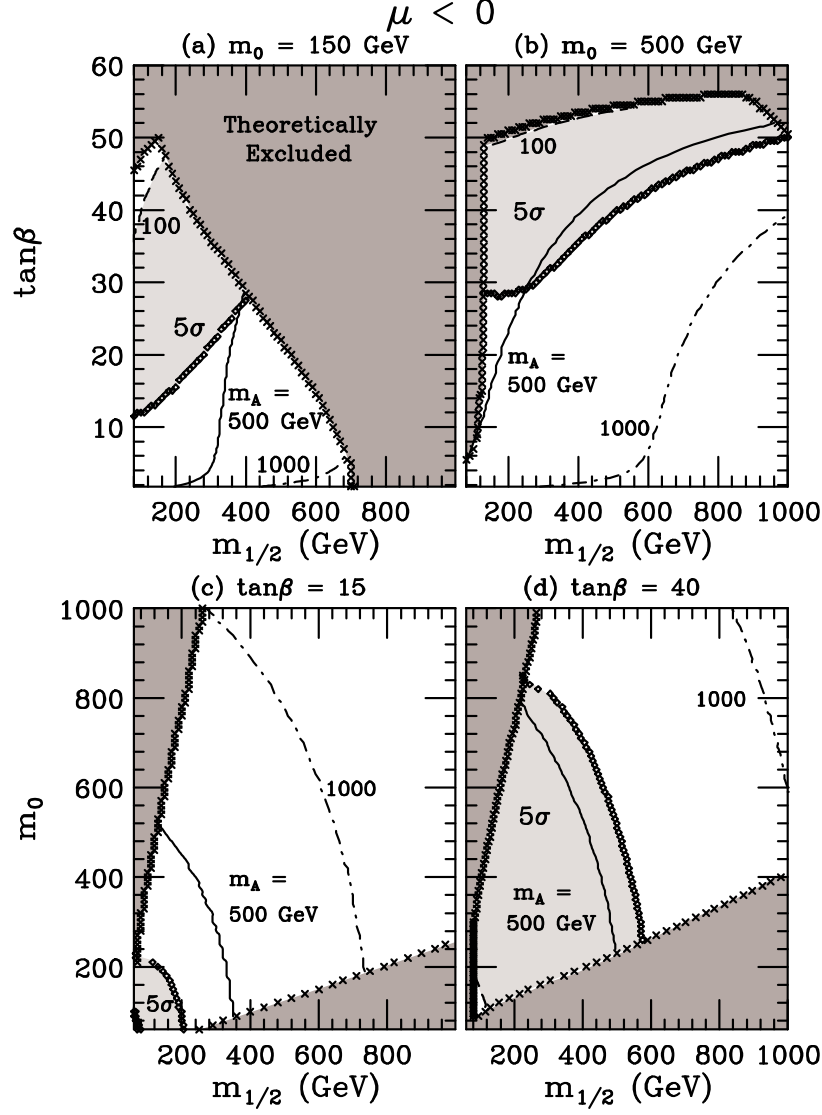


FIG. 4. The  $5\sigma$  contours at the LHC for an integrated luminosity ( $L$ ) of  $300 \text{ fb}^{-1}$  in (a) the  $m_{1/2}$  versus  $\tan\beta$  plane with  $m_0 = 150$  GeV, (b) the  $m_{1/2}$  versus  $\tan\beta$  plane with  $m_0 = 500$  GeV, (c) the  $m_{1/2}$  versus  $m_0$  plane with  $\tan\beta = 15$ , and (d) the  $m_{1/2}$  versus  $m_0$  plane with  $\tan\beta = 40$ . Also shown are the mass contours for  $m_A = 100$  GeV (dashed), 500 GeV (solid) and 1000 GeV (dot-dashed). The discovery region is the part of the parameter space with light shading. The regions with dark shading are the parts of the parameter space excluded by theoretical requirements. The region excluded by the  $m_{\chi_1^+} > 85$  GeV limit from the chargino search [35] at LEP 2 is indicated.